remote sensing

MDPI

Article

Predicting Grassland Fire-Occurrence Probability in Inner Mongolia Autonomous Region, China

Chang Chang [1,2], Yu Chang [1,*], Zaiping Xiong [1], Xiaoying Ping [3], Heng Zhang [4], Meng Guo [5] and Yuanman Hu [1,6]

1 CAS Key Laboratory of Forest Ecology and Management, Institute of Applied Ecology, Chinese Academy of Sciences, Shenyang 110016, China; changchang20@mails.ucas.ac.cn (C.C.); zaipingx@iae.ac.cn (Z.X.); huym@iae.ac.cn (Y.H.)
2 University of Chinese Academy of Sciences, Beijing 100049, China
3 School of Public Administration, North China University of Water Resources and Electric Power, Zhengzhou 450045, China; ping_xiaoying@163.com
4 College of Forestry, Inner Mongolia Agricultural University, Hohhot 010019, China
5 School of Geographical Sciences, Northeast Normal University, Changchun 130024, China
6 E'erguna Wetland Ecosystem National Research Station, Hulunbuir 022250, China
* Correspondence: changyu@iae.ac.cn; Tel.: +86-24-83970350

Abstract: Fires greatly threaten the grassland ecosystem, human life, and economic development. However, since limited research focuses on grassland fire prediction, it is necessary to find a better method to predict the probability of grassland-fire occurrence. Multiple environmental variables impact fire occurrence. After selecting natural variables based on remote sensing data and anthropogenic variables, we built regression models of grassland fire probability, taking into account historical fire points and variables in Inner Mongolia. We arrived at three methods to identify grassland fire drivers and predict fire probability: global logistic regression, geographically weighted logistic regression, and random forest. According to the results, the random forest model had the best predictive effect. Nine variables selected by a geographically weighted logistic regression model exercised a spatially unbalanced influence on grassland fires. The three models all showed that meteorological factors and a normalized difference vegetation index (NDVI) were of great importance to grassland fire occurrence. In Inner Mongolia, grassland fires occurring in different areas indicated varying responses to the influencing drivers, and areas that differed in their natural and geographical conditions had different fire-prevention periods. Thus, a grassland fire management strategy based on local conditions should be advocated, and existing fire-monitoring systems based on original meteorological factors should be improved by adding remote sensing data of grassland fuels to increase accuracy.

Keywords: grassland fire; fire drivers; fire predicting; vegetation index; meteorological factors; Inner Mongolia; geographically weighted logistic regression; random forest

Citation: Chang, C.; Chang, Y.; Xiong, Z.; Ping, X.; Zhang, H.; Guo, M.; Hu, Y. Predicting Grassland Fire-Occurrence Probability in Inner Mongolia Autonomous Region, China. *Remote Sens.* **2023**, *15*, 2999. https://doi.org/10.3390/rs15122999

Academic Editor: Carmen Quintano

Received: 13 April 2023
Revised: 17 May 2023
Accepted: 2 June 2023
Published: 8 June 2023

1. Introduction

Grassland ecosystems are precious natural resources and have crucial ecological functions, such as maintaining water, regulating local climate conditions, and providing food and herbs [1,2]. Fire is a common disturbance factor [3,4], and in a long-term evolutionary process, it establishes a harmonious and balanced relationship with grassland ecosystems. Fire promotes grassland regeneration, succession, species evolution, and biodiversity, becoming an integrated part of grassland ecosystems [5,6]. However, in the context of global climate change along with human activities, fire frequency is increasing and fire seasons are lengthening [7]. In many regions, fire increasingly impacts the resources for human well-being and functions in the ecosystem [8]. Frequent and uncontrollable grassland fires are sudden and highly destructive disasters that not only alter the structure, function, pattern,

and processes of the landscape, but also affect the carbon cycle in grassland ecosystems [9]. Moreover, fires pose threats to herdsmen's lives, infrastructures, and valuable grassland resources [10]. They result from a combination of numerous anthropogenic and natural factors [11]. The accurate prediction of the occurrence of grassland fires aids in locating high-risk areas for fire prevention and fire-fighting. Many studies of grassland-fire occurrence have been performed utilizing remote sensing methods; the main methods and their advantages and disadvantages are shown in Table 1. The first three methods in Table 1 make no predictions on a time scale, and the last method does not consider influence factors comprehensively enough. Nevertheless, the third method in Table 1 is employed for reference in this study. Furthermore, daily meteorological factors should be included in prediction models to solve the problem of time scale.

Table 1. Main remote sensing methods on predicting grassland fire occurrences.

Serial Number	Methods	Advantages	Disadvantages
1	Modeling based on meteorological data from meteorological satellites [12]	Study area with large scale estimation can be made	Limited accuracy
2	Builds the relationship between fire occurrence and soil moisture investigated by field measurement [13–15]	High accuracy	Time-consuming and laborious; only a small-scale estimation can be made
3	Evaluation based on meteorological data, fuel condition of MODIS Inversion and other social data [16,17]	Consideration from many aspects; improves the accuracy of prediction to some extent	Many kinds of data need processing
4	Monitoring vegetation moisture by time-series satellites [18]	Long-term fire risk assessment	Considers only moisture of vegetation

The prediction of grassland-fire occurrence needs to choose independent variables. With human population increase and the development of the social economy, factors affecting grassland fires are becoming more complex [19]. Among natural factors, meteorological ones are commonly treated as fire drivers [20] because climate/weather can influence fire occurrence, with drier environments in some mesic biomes usually displaying more fire activity than wetter ones [21]. Climate conditions are key factors for the condition of vegetation and the distribution of live fuel loads and exercise an important impact on grassland fires and their spread. The vegetation indices based on remote sensing are key indicators to reflect the vegetation condition. Some scholars added variables such as spring NDVI, autumn NDVI [22], the vegetation condition index (VCI) [23], and the percentage of grassland, shrubland, and forest areas [24] that can reflect the vegetation condition or fuel load in the analysis of fire occurrence patterns. In addition, topography influences fire occurrence indirectly by contributing to fuel changes and the moisture content by changes in temperature and water availability [25]. Although topography plays a relatively smaller role on fire-occurrence patterns, researchers have nevertheless opted to select variables such as a topographic roughness index, considering elevation, slope, aspect index, and surface curvature in fire-occurrence predictions [26]. Human activity is always the major factor; for example, higher human population density always increases ignition sources [27] because of smoking, outdoor barbecues, vehicle breakdown, and other human activities. The distance to the nearest road and settlement is often used as a proxy for the intensity of human activities [28]. Alongside the chosen variables, appropriate models are also needed to predict grassland fire occurrences.

Over the last decades, many regression models have been developed to explore the relationship between fire occurrence and independent variables [20,29–31]. Among these, the global logistic regression (GLR) model is the most widely used conventional method [32]. GLR assumes that the samples are independent and have a constant relationship between the dependent variable and the independent variables in the entire study area [33]. However, due to the environmental heterogeneity in different spatial

locations, the relative importance of factors affecting fire occurrence may inevitably be different. This phenomenon is called spatial non-stationarity [34]. To solve this problem, the geographically weighted logistic regression (GWLR) model was adopted. This model can deal with the various relationships between dependent and independent variables across geographical locations [35]. GWLR first assumes that the model structure is spatially non-stationary, which means that the relationship between the binary-dependent variables and the continuous independent variables changes with geographic locations. Second, it tests whether the spatial non-stationary relationship of this hypothesis is significant [34]. Recently, to improve prediction accuracy, a variety of machine-learning methods, including neural networks, support vector machines, and random forests [31,36,37] also have been used in fire-occurrence prediction. Among these methods, Random Forest (RF) is deemed to be a flexible method to assess complex interactions among variables. With this method, it is unnecessary to set the function form in advance, and the important variables are automatically selected, regardless of how many are input at the beginning. It can overcome the problem of over-fitting [20,32] and the complex interactions between covariables to obtain a high predictive performance [38]. Therefore, the RF model has demonstrated its strong predictive ability in fire-occurrence probability [20,39].

Although GWLR overcomes the shortcomings of GLR and new machine-learning methods have been proposed, model comparisons are commonly taken to determine the best-fitted model in fire prediction [8,40]. For example, Guo (2016) and Oliveira (2012) both compared the GLR model to the RF model in fire predictions and found that the RF model performs better than the GLR model. Because RF can generate multiple prediction models at the same time and summarize the results of the models to improve the accuracy of classification, it is more accurate than GLR [20,39]. Phelps and Woolford employed logistic regression, bagged classification trees, random forest, and neural network,, but they found all the models were unsuitable for fire-occurrence prediction because of the bias in their training data, which led all the models to overpredict the number of fire occurrences [40]. However, in the present study, multiple fire-predicting models focus on the spatial differences of fire occurrence [24,41,42] rather than the variation within the year. Furthermore, research has focused more on forest-fire occurrence [43–46] and less on grassland fires, even though both are important vegetation ecosystems on the earth. Moreover, grasslands cover one-third of the Earth's terrestrial surface [47], so the impact of grassland fires cannot be neglected. China possesses nearly 3.92×10^6 km^2 area of grasslands, accounting for 12% of the world's grasslands and 41.7% of the national land area. Grassland is the main land cover type in the Inner Mongolia Autonomous Region [48]. Meanwhile, the Inner Mongolian grassland is the main component of the temperate grasslands of Eurasia, where grassland fires are extremely active [49]. To protect grassland ecosystems, safeguard the lives and safety of local people, and promote the development of husbandry, it is necessary to explore the rules of grassland fire-occurrence distribution in Inner Mongolia. Due to the lack of relevant research, the driving factors and spatial patterns of grassland fires in Inner Mongolia are currently unclear.

In this study, we aim to (1) explore the temporal and spatial distribution patterns of historical grassland fires from 2000 to 2018 in Inner Mongolia to obtain a whole view of the distribution of fire points; (2) predict grassland fire probability based on fire points and environmental variables by three models to identify the drivers of grassland fire occurrence and thereby to find the best-fitting model by comparing the performances of all three; (3) apply the three models to check whether they can predict the daily probability of grassland-fire occurrence in Inner Mongolia in 2014 accurately and put forward some suggestions on grassland-fire management. Our results will facilitate formulating region-specific strategies for protecting grassland resources, and forecasting, warning of, and managing fires.

2. Materials and Methods

2.1. Study Area

The Inner Mongolia Autonomous Region is located in the north of China (37°24′–53°23′N, 97°12′–126°04′E), bordered by Mongolia and Russia. The distance from the east to the west is about 2400 km, and the span between the north and the south is about 1700 km. The region has a long and narrow shape extending from the northeast to the southwest with a total area of 118.3 × 10^4 km^2 (Figure 1a). According to the Seventh National Census of China in 2020, the resident population of the district was then 24.05 million.

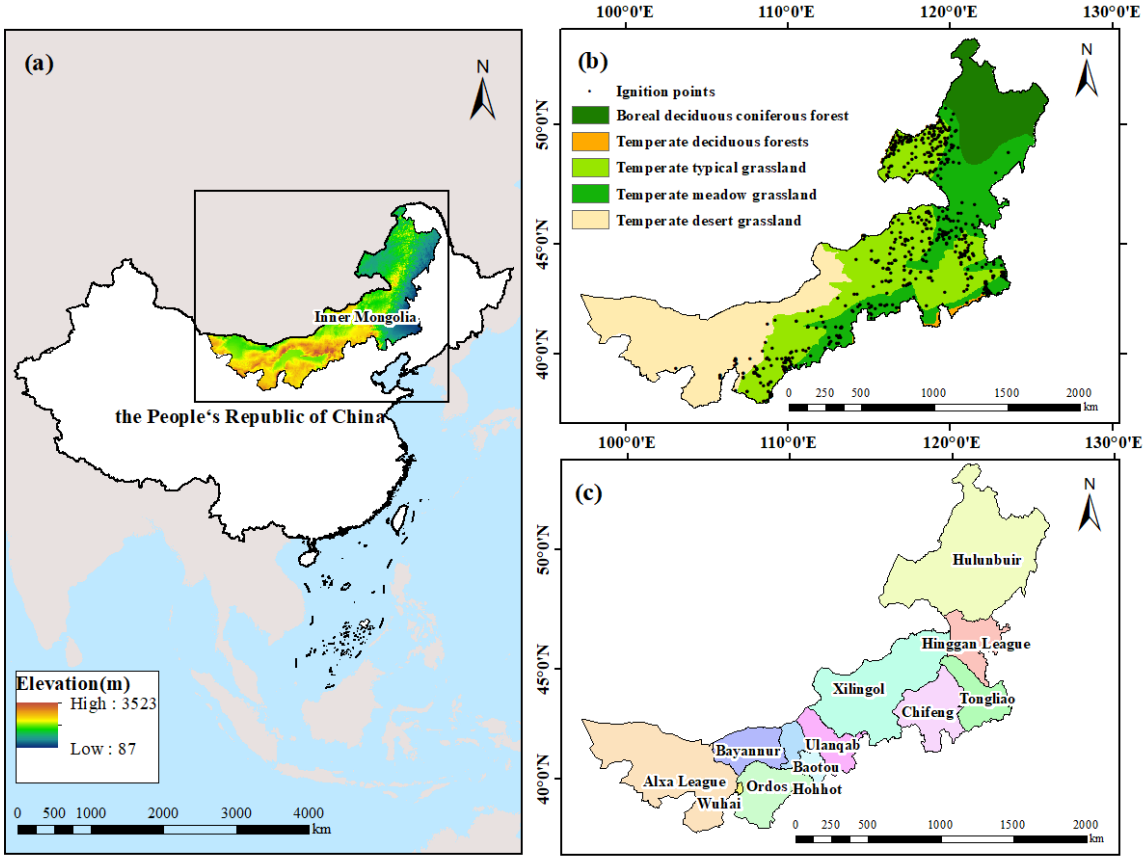

Figure 1. Geographical location of the study area. (**a**) The relative position and elevation of Inner Mongolia, (**b**) fire ignition points and vegetation type map, and (**c**) administrative map on the city level. (All the base map layers except ignition points were from © Institute of Geographic Sciences and Natural Resources Research, CAS; fire ignition points came from Inner Mongolia Fire Management Department).

Inner Mongolia has a temperate continental monsoon climate with the annual average temperature ranging from 0 to 8 °C and annual precipitation from 50 to 450 mm [50]. The climate is characterized by large temperature differences, long sunshine duration, and limited and imbalanced precipitation. From the northeast to the southwest, it comprises temperate humid, semi-humid, semi-arid, arid, and extreme arid zones [51].The grassland vegetation in Inner Mongolia has a distinct zonal distribution pattern from northeast to southwest as well. The three main types are temperate meadow grassland, temperate typical grassland, and temperate desert grassland [52] (Figure 1b).

2.2. Data Sources and Pre-Processing

2.2.1. Dependent Variable

We collected the historical grassland fire-occurrence records from the Inner Mongolia Fire Management Department. These records contained detailed information on

each grassland fire in Inner Mongolia, including the geographical location, the start time, size, cause, and casualties. There were 1049 fires recorded from 2000 to 2018, of which 685 had geographical coordinate information; thus we selected these records and removed the ones without geographical information. The geographical distribution patterns of fire occurrences are shown in Figure 1b. Binomial LR, GWLR and RF models were adopted in this study. Because the two binomial models required the data in a binomial distribution [53], and the RF model also needs a classified variable as a dependent variable, a certain percentage of randomly distributed non-fire points had to be created to meet the requirements [54]. Then, based on the 685 fire-occurrence points, the non-fire-occurrence points were created by ArcGIS10.6 with 1.5 times number of fire points [55]. Therefore, 1711 was the total number of sampling points. Next, we created an attribute for these points in the attribute table, with the non-fire points coded 0 and the fire points coded 1. We treated this attribute as the dependent variable. The specific workflow is presented in Figure 2.

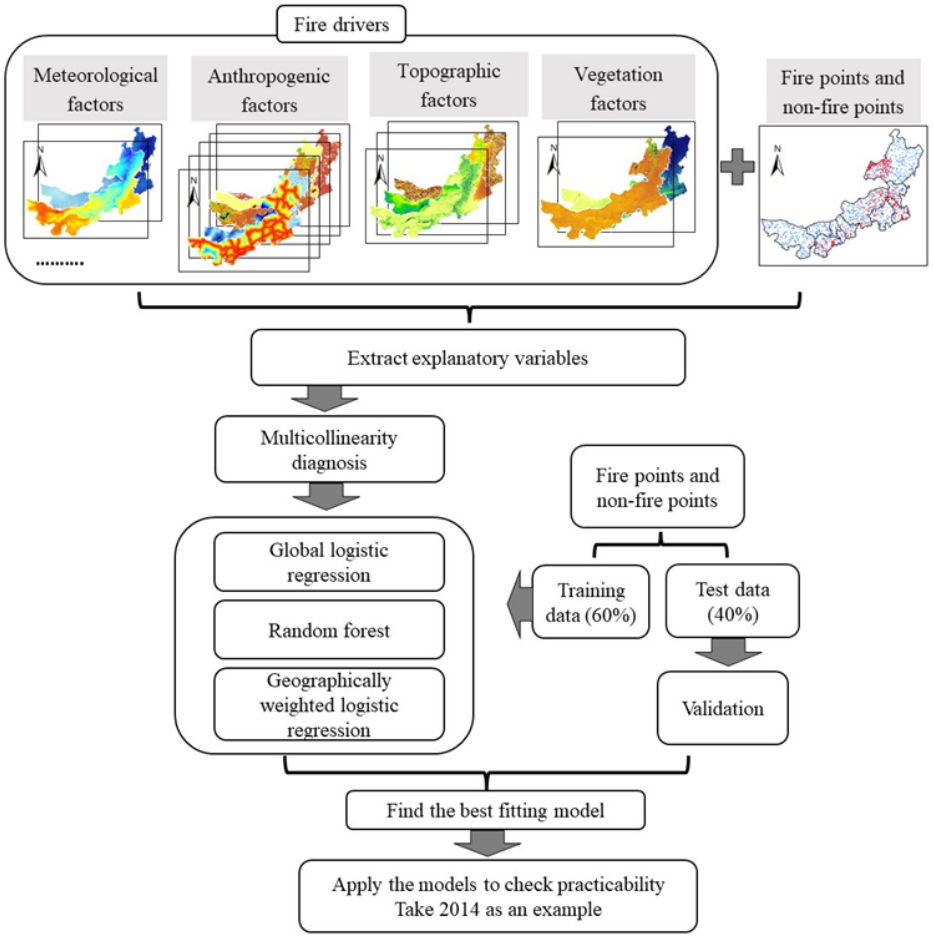

Figure 2. Flowchart of predicting the probability of grassland-fire occurrence.

2.2.2. Explanatory Variables

The drivers of fire occurrence are various, including anthropogenic and natural factors [11]. Human actions usually are an ignition trigger, while natural environmental factors influence fire-occurrence probability. Some factors can be biotic, such as the vegetation cover influencing the load and flammability, or abiotic, such as the climate and topography influencing fuel moisture and fire spread [56–58]. Therefore, we chose four categories (meteorology, anthropogenic activity, vegetation, and topography) as explanatory variables to predict fire-occurrence probability. The meteorological factors included mean annual temperature and precipitation, daily average wind speed, daily average temperature, daily average specific humidity, and daily cumulative precipitation; the anthropogenic factors

involved population density and distance to the nearest settlement, road, river, and railway. Vegetation factors included the Normalized Difference Vegetation Index (NDVI) and the global vegetation moisture index (GVMI), while the topographic factors consisted of elevation, aspect and slope. These choices will be explained in the following paragraphs. The data source, abbreviation, and unit of all the variables are listed in Table 2.

- Meteorological factors

Meteorology plays an important role in fire occurrence. The mean annual temperature and precipitation were selected as climate factors because they have an obvious influence on fuel moisture content, a crucial condition for fire occurrences. Furthermore, they are traditional indicators of the degree of climate change [59]. The daily average temperature, windspeed, specific humidity, and cumulative precipitation directly influence the moisture content of fuels [60]. Meteorological factors in this study are from the China Meteorological Forcing Data (1979–2018) [61]. These CMFD are derived from remote sensing products, reanalysis datasets, and in situ station data, providing the NetCDF format of the dataset. The value of each variable was extracted by the locations and date of the sampling points. For non-fire points, the daily meteorological data consisted of a random date from 1990 to 2018 extracted three times to build models to obtain the prediction accuracies. We found a negligible difference in accuracy among the three models.

- Anthropogenic factors

Human activities are closely related to human-caused fire occurrences [62]. The distance to human infrastructure, such as roads, railways, and settlements, is usually used to represent the intensity of human activity [28,63]. In Inner Mongolia, herdsmen prefer to water their livestock from rivers, so the closer the river, the greater the intensity of human activity. Based on this, we selected the distance to the nearest settlement, road, railway, and river as the anthropogenic factor. Digital maps (1:250,000) locating these points were collected from the National Catalogue Service for Geographic Information. We calculated the Euclidean distance to the nearest railway, road, river, and settlement, respectively, to create four raster layers by ArcGIS. These distances served as proxies of intensity for human activities. Next, the total sampling points layer was superimposed on the four layers, respectively, and we extracted the values of the four variables according to the location of points. Population density showed a strong correlation with the intensity of human activity, for the greater the population density in a region, the greater the number of people, so the more human activities [63]. Therefore, we used population density data of counties throughout the study area to generate the raster layer of population density, and then the total sampling points layer was superimposed on this layer to extract the population density value as the population density variable.

- Vegetation factors

Fire needs fuel to burn, and the fuel load also influences the fire occurrences. Vegetation coverage is usually used to indicate the gross of live and dead fuels above the surface [64]. The Normalized Difference Vegetation Index (NDVI) can be used to represent the vegetation coverage [65]. The vegetation moisture content is also one of the conditions of vegetation flammability. The Global Vegetation Moisture Index (GVMI) can provide direct information on vegetation water content at the canopy level [66] and thus reflects the moisture content of live fuels. Therefore, two indexes, NDVI and GVMI, were selected to represent the fuel load and fuel moisture conditions, respectively. The NDVI raster dataset from the Resource and Environment Science and Data Center was obtained to calculate the average NDVI value from 2000 to 2018, utilizing the Raster Calculator tool in ArcGIS10.6 to create an NDVI raster layer. Next, the total sampling points layer was superimposed on the NDVI raster layer to extract values as a variable GVMI is based on a combination of near-infrared and short-wave infrared bands of the electromagnetic spectrum to estimate vegetation moisture content (Ceccato et al., 2002). Bands 2 and 6 of the product MOD09A1 of MODIS surface reflectance were used.

- Topographic factors

The topographic factors affect vegetation distribution, composition, and flammability [67]. The higher the elevation, the lower the temperature. Different aspects will receive imbalanced radiation from the sun. Hence, the vegetation type changes with elevation and aspect. Human-caused fires occur more frequently on gentle slopes [68]. The elevation data came from the Geospatial Data Cloud. The 90 m spatial resolution digital elevation model (DEM) was adopted [69], and then the processes of georeferencing, mosaic, clip, and resampling on DEM were necessary. By utilizing the 3D Analyst tool of ArcGIS10.6, the raster layers of the slope and aspect were obtained. The aspect needed to be exponentiated before analysis, so it was converted into an aspect index according to the specific method provided by Zhangwen Su [26].

Explanatory variables were extracted from the corresponding map layers, and the value of each was extracted as an attribute of the sampling points to form the completed sampling dataset collection. We randomly chose 60% from fire points and non-fire points respectively as a training dataset, and the remaining 40% as a test dataset.

Table 2. Explanatory variables and their sources.

Factors	Variables	Abbreviation	Data Source	Units	Resolution
Meteorological factors	Mean annual temperature	Temp	China Meteorological Forcing Data (1979–2018) [61]	K	0.1°
	Mean annual precipitation	Prec		mm/h	0.1°
	Daily average specific humidity	Humi_dy		kg/kg	0.1°
	Daily cumulative precipitation	Prec_dy		mm/h	0.1°
	Daily average temperature	Temp_dy		K	0.1°
	Daily average wind speed	Wind_dy		m/s	0.1°
Anthropogenic factors	Distance to nearest settlement	D_resp	National Catalogue Service for Geographic Information https://www.webmap.cn (accessed on 21 May 2021)	km	500 m
	Distance to nearest road	D_road		km	500 m
	Distance to nearest river	D_river		km	500 m
	Distance to nearest railway	D_rail		km	500 m
	Population density	P_density	National Bureau of Statistics of China http://www.stats.gov.cn (accessed on 12 February 2021)	per/km^2	500 m
Vegetation factors	Global vegetation moisture index	GVMI	Level-1 and Atmosphere Archive & Distribution System Distributed Active Archive Center https://ladsweb.modaps.eosdis.nasa.gov/ (accessed on 22 April 2021)	-	500 m
	Normalized Difference Vegetation Index	NDVI	Resource and Environment Science and Data Center [70]	-	1000 m
Topographic factors	elevation	Elev	Geospatial Data Cloud http://www.gscloud.cn (accessed on 16 April 2021)	Meter	500 m
	aspect index	Aspect		-	500 m
	slope	Slope		degree	500 m

2.3. Data Analysis Methods

2.3.1. Multicollinearity Diagnosis between Explanatory Variables

If there is a strong multicollinearity among explanatory variables, the regression fitting may produce a biased parameter estimation, leading to an excessive standard error of regression coefficient; thus, the model will be unreliable [53,63]. The variance inflation factor (VIF) is a common method to evaluate multicollinearity among variables. Therefore, we did a multicollinearity diagnosis for our sampling dataset by VIF. The VIF test was manipulated by the car package of R studio 1.3. This indicated that there was moderate collinearity for the Prec variable and the NDVI variable with their VIF greater than 5 (Figure 3).

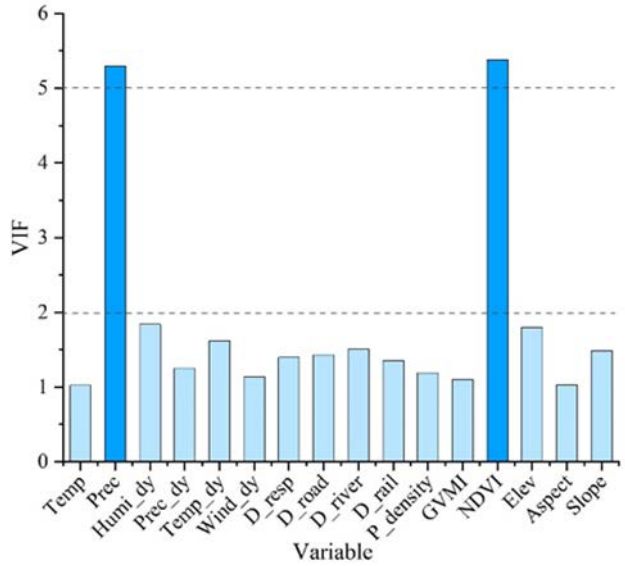

Figure 3. The VIF values of every explanatory variable (If VIF > 10, there is severe collinearity; 5 < VIF < 10, there is moderate collinearity; 2 < VIF < 5, there is mild collinearity [66]).

2.3.2. Trend Analysis of Grassland Fires

To obtain a concrete and overall distribution of all the historical fire occurrence points, we need a tool to present them clearly. Trend analysis is an analytical tool in the ArcGIS geographic statistics module, one that can analyze the spatial distribution trends of data [71]. To find the spatial distribution patterns of grassland-fire occurrences, the Inner Mongolia map was divided into 6064 grids of 20 × 20 km by the create fishnet tool; then the fire points in each grid were calculated. Trend analysis in ArcGIS was used to obtain a three-dimensional overview of fire points in the geographical space. Further, to find the characteristics of time change in a year, a month was divided into 2 parts; thus, a year was divided into 24 parts. The sample number of fire points was reclassified into 24 parts according to the fire-occurrence date from 2000 to 2018.

2.3.3. Modelling Methods

In this study, we selected the logistic regression model as a benchmark and the random forest model for its strong predictive ability in fire-occurrence probability [39]. We selected geographically weighted logistic regression, which demonstrates its ability for dealing with spatial heterogeneity. The following reveals how we employed the three models.

- Global logistic regression (GLR)

Logistic regression is a useful tool for predicting a binary variable through a series of continuous or categorical predictor variables. In our study, the binary variable was whether the fire happened at the sampling points, so the explanatory variables were used to explain the binary variable. However, the variable of Prec has been diagnosed as demonstrating moderate collinearity with NDVI and was thus deleted from explanatory variables. The training dataset was input to build the model, and the test dataset was used to calculate the prediction accuracy. The global logistic regression was performed by the AER package in R studio1.3.

- Geographically weighted logistic regression (GWLR)

The GWLR model can be built by the spgwr and GWmodel packages in R, ArcGIS, GWR4 software, etc. However, among these models, the freely accessible GWR4 software has a strong operability by providing a concise workspace, making it easy to select the model type, input the variables, and output the results. As noted above, the training dataset was also utilized to build the GWLR model. With the Prec deleted, the test dataset

was used to test the model performance. A conventional GWR is represented by the following expression:

$$y_i = \sum_k \beta_k(a_i, b_i)x_{k,i} + \varepsilon_i \quad (1)$$

where y_i, $x_{k,\mathrm{i}}$ and ε_i are dependent variables, k is the explanatory variable, and the Gaussian error is at location, respectively; (a_i, b_i) is the X/Y coordinate of the i location; and coefficients β (a_i, b_i) vary, depending on the location.

We employed the GWR4 software to build the GWLR model and chose the adaptive bisquare as the kernel function type, and the golden section search as the bandwidth selection method. The "golden section search" option can be used to automatically determine the best bandwidth size. Generally, the fixed kernel specifies an equal distance threshold for each regression point, while the adaptive kernel specifies the number of neighbors to be considered for each regression point. Therefore, the fixed kernels approach is suitable when the points are regularly distributed in space, and the adaptive approach is more appropriate for spatially clustered points [72]. According to the spatial distribution pattern of our fire occurrence data, the adaptive approach was selected to build the model. The Akaike information criterion (AIC) approach was used to assess the goodness-of-fit for each model. GWLR shares similarity with its global counterpart, producing the regression coefficients and significance tests. It is worth noting that rather than a single parameter, a collection of parameters for each sampling point can be obtained [34].

- Random forest (RF)

In the RF model, the parameter of mtry represents the number of variables used to split the tree at every node, while the ntree parameter represents the number of decision trees, and the nodesize parameter represents the minimum number of nodes in a decision tree [73]. According to our data, we performed the parameter tuning, and mtry defaulted to "2", while Nodesize defaulted to "1" for our classification model. The ntree was determined by multiple testing for how many decision trees should be obtained when the error in the model is relatively stable. After multiple tests, the parameter of ntree was set as 500.

To understand the importance of each variable in the model, this study utilized IncNodePurity, which provides a means to assess the contribution of each predictor variable to the modelling performance. The value is just relative and can be calculated using the decrease in tree-node impurities attributable to each predictor variable [73]. A larger IncNodePurity indicates a stronger importance of these predictor variables [74]. Furthermore, the RF model has the limitation that it is unable to calculate the specific regression coefficient and confidence interval. We utilized the randomForest package in R studio4.0.3 to build the random forest model.

2.3.4. Model Evaluation Methods

To evaluate the goodness of fit for the three models we chose forr statistical measures, we selected the Akaike information criterion (AIC), the area under curve (AUC), the mean absolute error (*MAE*), the root mean square error (*RMSE*), and R^2. Based on the concept of entropy, AIC can measure the complexity of the estimated model and the goodness of fit for the model-data. AIC is an index obtained in the process of model fitting. The characteristic receiver-operating curve (ROC) was obtained by plotting sensitivity versus specificity for various probability thresholds. The area under the curve (AUC) is often also used to evaluate model performance [75]. *MAE*, the average value of absolute error, can better reflect the actual situation of the predicted value error. *MAE* is defined in the following expression:

$$MAE = \frac{1}{n}\sum_{i=1}^{n}|\hat{y}_i - y_i| \quad (2)$$

RMSE is adopted to measure the deviation between the observed value and the true value. It is more sensitive to outliers than *MAE*.

$$RMSE = \sqrt{\frac{1}{n}\sum_{i=1}^{n}(\hat{y}_i - y_i)^2} \quad (3)$$

R^2 reflects the fitting degree of the regression line to the observed value, and is calculated by the following equation:

$$R^2 = 1 - \frac{\sum_{i=1}^{n}(\hat{y}_i - y_i)^2}{\sum_{i=1}^{n}(\hat{y}_i - \overline{y}_i)^2} \quad (4)$$

where n is the number of samples, $\hat{y}_i$ is the fire-occurrence probability predicted by the model, y_i is a binary value representing whether a fire exists, and $\overline{y}_i$ is the arithmetic mean of binary values.

3. Results

3.1. Temporal and Spatial Distribution Patterns of Fire Occurrences

From a spatial perspective, the distribution of fire points demonstrated a decreasing trend from east to west. The distribution was more balanced from the north-south direction, except for the northernmost area, where no fire points existed due to the lack of grassland (Figure 4).

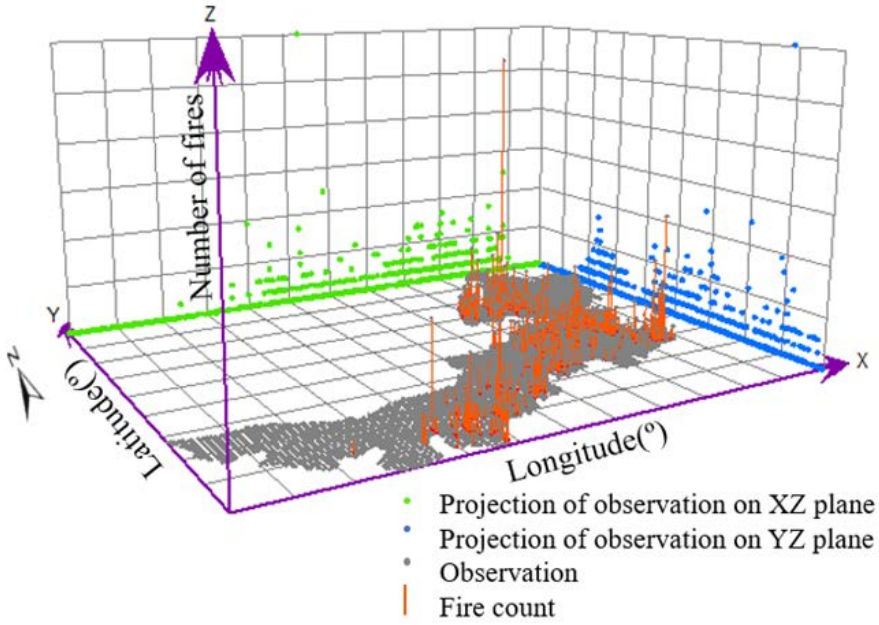

Figure 4. The spatial distribution of grassland fires in Inner Mongolia from 2000 to 2018. (The height of orange lines represent the number of fires; the grey points are the position of the observation point and the projection on the XY plane. The green points are the projection of the observations on the XZ plane; the blue points are the projection of the observations onto the YZ plane).

From a temporal perspective, there were two peaks of fire occurrences during a year. The first one appeared in the first half of April, and the second, in the first half of October (Figure 5). The number of fires during the first fire-prevention period was significantly higher than during the second fire-prevention period. According to the Regulations on Fire Prevention of Forests and Grasslands in the Inner Mongolia Autonomous Region, there are two fire prevention periods, 15 March–15 June, and 15 September–15 November. We found that the periods when the number of fires was greater than 20 coincided with the fire-prevention periods regulated in the region.

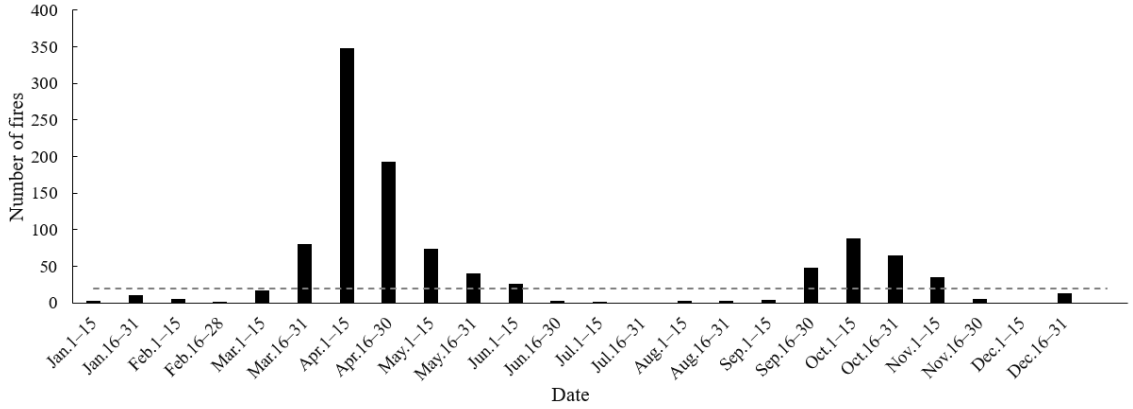

Figure 5. Changes of the number of grassland fires in Inner Mongolia at the half-month interval. The grey dotted line represents 20 fires.

3.2. Model Fitting

Based on the GLR model, only 9 variables had significant coefficients ($p < 0.05$) among the 16 explanatory variables: namely, Temp, Humi_dy, Wind_dy, D_river, D_resp, D_rail, GVMI, NDVI, and Slope were regarded as grassland-fire drivers. Among the drivers, only NDVI and Wind_dy were positively correlated with fire occurrences, and the rest of drivers were negatively correlated (Table 3).

Table 3. Parameter estimation of explanatory variables by the GLR model.

Variable	Abbreviation	Coefficient	Standard Error	*p*-Value
Intercept	Intercept	38.543	10.218	<0.0001
Mean annual temperature	Temp	−0.138	0.036	<0.0001
Distance to nearest river	D_river	−0.009	<0.0001	<0.0001
Distance to nearest settlement	D_resp	−0.142	<0.0001	<0.0001
Distance to nearest railway	D_rail	−0.004	<0.0001	0.024
Global vegetation moisture index	GVMI	−7.523	1.650	<0.0001
Normalized Difference Vegetation Index	NDVI	2.599	0.560	<0.0001
Daily average specific humidity	Humi_dy	−857.033	81.818	<0.0001
Daily average wind speed	Wind_dy	0.217	0.050	<0.0001
Slope	Slope	−0.108	0.024	<0.0001

The drivers selected by the GWLR model were consistent with the GLR model. The GWLR model spatialized the coefficient of each of the selected explanatory variables (Figure 6), which demonstrated large spatial variations (Table 4).

Table 4. Coefficient statistics of explanatory variables selected by the GWLR model.

Variable	Mean	Min	1Q	Median	3Q	Max
Intercept	30.55973	8.352316	14.07005	28.78026	40.13325	109.0789
Humi_dy	−711.947	−1407.05	−1115.85	−1037.32	−26.1174	262.0729
Wind_dy	0.204153	−0.37813	−0.21256	0.123083	0.534187	1.327401
NDVI	1.294488	−1.53458	0.749144	1.351105	1.899675	4.123084
GVMI	−7.48481	−9.86252	−8.10707	−7.24877	−6.92158	−3.26509
Temp	−0.10685	−0.38292	−0.14078	−0.09896	−0.0535	−0.02163
Slope	−0.06249	−0.10811	−0.0675	−0.0622	−0.05487	−0.03551
D_rail	−0.00752	−0.0189	−0.01085	−0.00803	−0.00173	−0.00097
D_resp	−0.11175	−0.25096	−0.14876	−0.12328	−0.05028	0.016634
D_river	−0.00949	−0.02133	−0.0166	−0.00881	−0.00415	0.002383

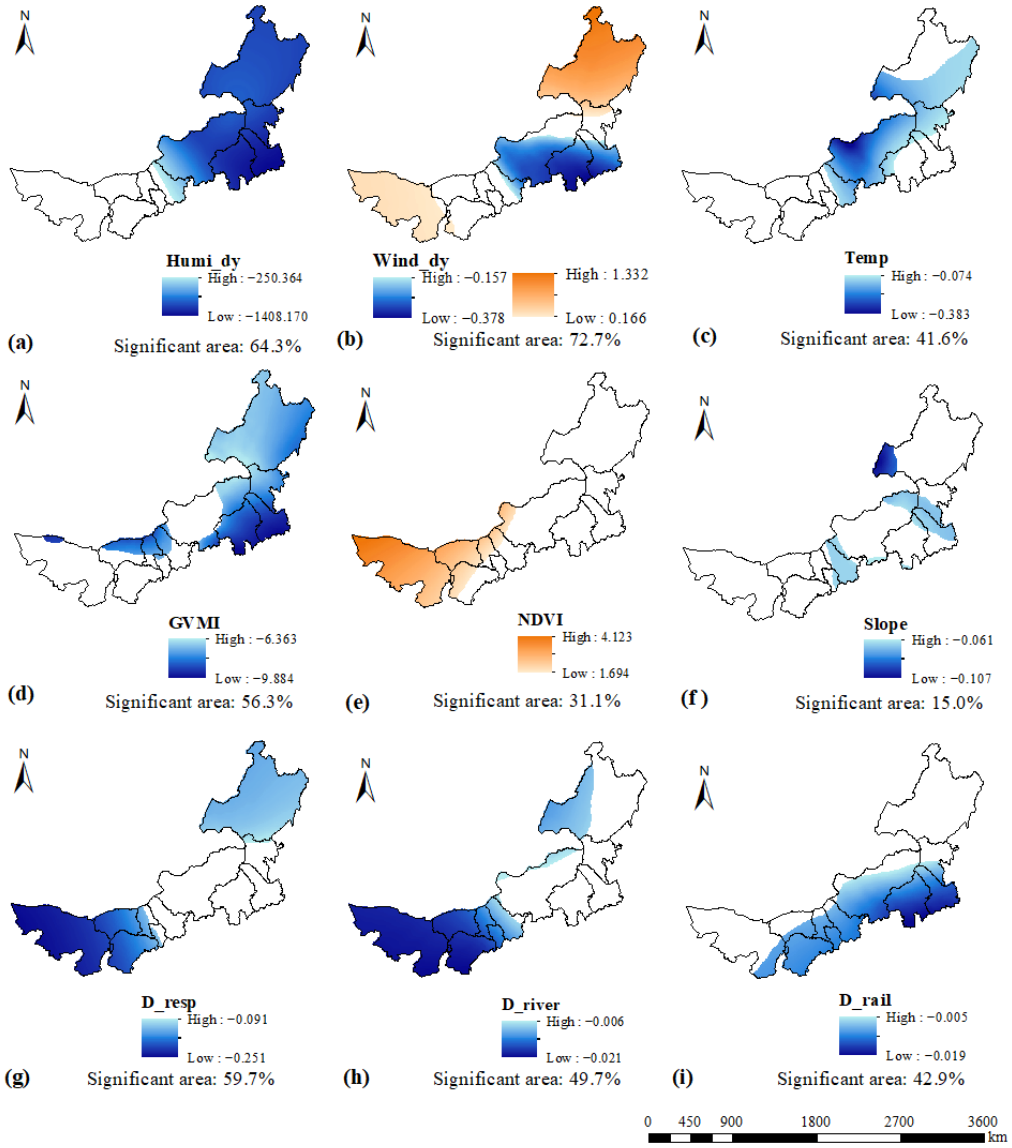

Figure 6. The spatial distribution of significant areas of the estimated coefficient for each variable selected by GWLR model. These maps were drawn according to the *t*-value for each pixel. The pixels with the corresponding *t*-value between −1.96 and 1.96 (insignificant area) are not displayed on the graph. Those pixels with the *t*-value greater than 1.96 or less than −1.96 (significant area) are displayed on the graph. The negative coefficient values are depicted in cool colors, and the positive coefficient values are depicted in warm colors. (**a**) is the spatial distribution of significant areas of the estimated coefficient for Humi_dy, (**b**) is for Wind_dy, (**c**) is for Temp, (**d**) is for GVMI, (**e**) is for NDVI, (**f**) is for Slope, (**g**) is for D_resp, (**h**) is for D_river and (**i**) is for D_rail.

Among the meteorological factors, the significant area of Humi_dy was distributed in the eastern and central parts of the study area, accounting for more than 64.3% of the total. In the positively significant area of Wind_dy located in the northernmost and westernmost area, including Hulunbuir and almost the entirety of Alxa, the negatively significant areas are concentrated in the middle. Temp was significant in some parts of the east, showing a negative correlation. Among the vegetation factors, GVMI was more significant in the eastern region, with small areas distributed in the central and western regions. NDVI was positively significant correlated with fire occurrence in a small area in the west. As for the topographic factors, only Slope was negatively correlated with a significant area, accounting for only 15% of the study area scattered in the eastern and central regions. Among anthropic factors, the significant area of D_resp was found in Hulunbuir and

the western region, with a greater impact on fire occurrences in the west. D_river was significantly negatively correlated in the west of Inner Mongolia and west of Hulunbuir. The significant area of D_rail was located in southern Inner Mongolia.

All the explanatory variables were put into the RF model. To understand the importance of each variable in the model, the IncNodePurity was employed. The ranking of variables is shown in Figure 7. In general, the importance of each explanatory variable was quite different, with the two daily-scale meteorological variables, Humi_dy and Temp_dy, much greater than other variables. Five meteorological variables stood in the top six in importance, indicating that meteorological conditions were the main cause of the grassland-fire occurrences. The importance of the NDVI variable reflecting the load of fuels was relatively high, as expected. Among the three topographical variables, Slope and Aspect were of lower importance, indicating that topographical conditions have less impact on the occurrence of grassland fires in Inner Mongolia.

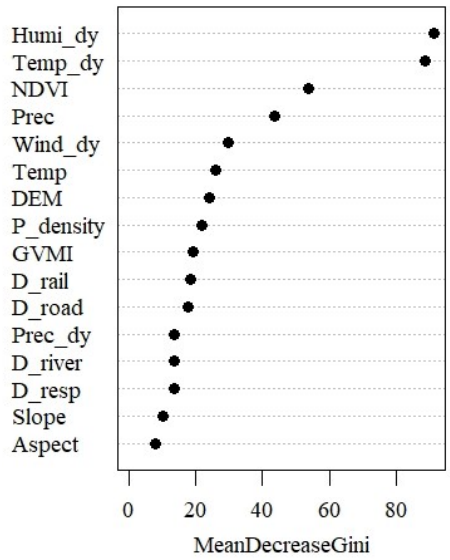

Figure 7. The importance ranking of the explanatory variables in RF model.

3.3. Model Validation

Table 5 lists several statistical measures to evaluate the performance of the GLR, GWLR and RF models. The RF model as a machine-learning algorithm cannot obtain the AIC value, so only the GLR and GWLR models were compared according to AIC. The AIC value of the GWLR model was smaller than that of the GLR model. This indicated that the GWLR model had a higher goodness of fit. The AUC value of GLR, GWLR and RF model was 0.841, 0.909 and 0.944; the *MAE* value was 0.148, 0.111 and 0.053; the *RMSE* value was 0.390, 0.338, and 0.231; R^2 was 0.363, 0.537, and 0.779, respectively. The higher R^2 and AUC values mean higher prediction accuracy, while on the contrary, the lower MAE and *RMSE* values represent a superior fit of the models. Therefore, the RF model has the highest scores in the AUC and R^2 and the lowest with *MAE* and *RMSE*. In comparison, the RF model performed better than both the GWLR and the GLR model and had the ability to predict grassland-fire occurrences in the region more accurately.

Table 5. Comparisons of the quality of fit of the three models by test dataset.

Model	Akaike Information Criterion (AIC)	Area under Curve (AUC)	Mean Absolute Error (*MAE*)	Root Mean Square Error (*RMSE*)	R^2
GLR	1018.496	0.841	0.148	0.390	0.363
GWLR	807.330	0.909	0.111	0.338	0.537
RF	-	0.944	0.053	0.231	0.779

3.4. Model Application

According to the RF model, daily meteorological conditions were of higher importance than other explanatory variables. The vast territory of Inner Mongolia and its geographical features lead to great spatial variations in the meteorological conditions, resulting in greater differences in the probability of fire occurrence in the eastern and western regions. Therefore, we randomly chose two points, one in the eastern and the other in the western area. Point 1 was located in the Hulunbuir grassland in northeastern Inner Mongolia, and Point 2 was located in the Ordos Plateau. Both points were areas with a high density of historical fire points. Based on the 19-year fire records obtained, we found that 2014 had the highest number of grassland fires, with a total of 111 occurrences. For this reason, 2014 served as an example. We used the three models to estimate the probability of fire occurrence with daily meteorological variables in 2014 and other explanatory variables.

Figure 8a shows the estimated probability of fire occurrence according to the three models at Point 1, and Figure 7c, at Point 2 on each day in 2014. We found that the estimated probability of fire occurrence with GLR and GWLR was higher than with RF at both locations. During periods with no fire prevention, the probability according to GLR and GWLR was also much higher than with RF, indicating that the RF model reasonably assesses fire prevention periods. We also found that the probability of fire occurrence estimated by each model at Point 1 was higher than at Point 2, which may be due to higher fuel loads at the former.

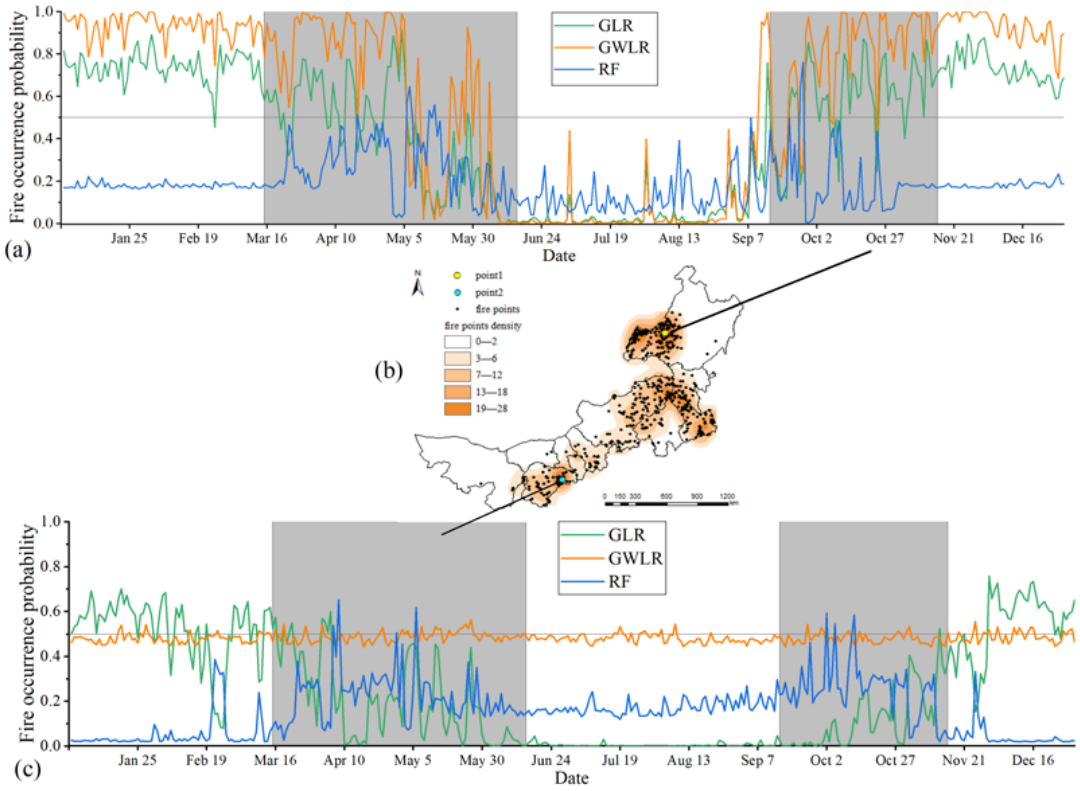

Figure 8. The fire-occurrence probability of two typical points in Inner Mongolia in 2014. (**a**,**c**) are the daily fire-occurrence probability of two typical points in 2014. The gray area represents the fire-prevention periods, and the gray lines indicate the value of 0.5; (**b**) is the kernel density level of historical grassland-fire occurrences.

4. Discussion

4.1. Temporal and Spatial Distribution Patterns of Historical Grassland Fires

In space, fires were historically densely distributed in eastern and central Inner Mongolia because these are areas of typical grassland and meadow grassland (Figure 1b) that provide sufficient fuel. Furthermore, these areas have dense traffic routes, and human ac-

tivities are more intense than in western Inner Mongolia. In the northern part of Hulunbuir, the main vegetation type is boreal deciduous coniferous forest (Figure 1c), so grassland fires rarely occur. Historically, fires are concentrated in spring and autumn (Figure 5) and thus closely related to local climate characteristics. The area is dominated by a temperate continental monsoon climate [76]. In spring, the temperature rises rapidly, the wind speed is high, and the air humidity is low, leading to frequent fires. In autumn and winter, the air is dry, increasing the number of fires. However, because of the high latitude, snow-covered dead fuel in winter reduces the probability of fire occurrence [77].

4.2. Model Validation

According to the value of R^2 and AIC, the GWLR model fits better than GLR. The latter predicts fire occurrence in view of the different roles of variables across various spatial locations and thus produces lower values of *MAE* and *RMSE* and higher values of AUC than GLR (Table 5). This demonstrates that the GWLR model is more suitable to this study area than GLR because Inner Mongolia has a large area with strong heterogeneity.

Compared with the GWLR and GLR models, the RF model shows the best fitting and lowest values of *MAE* and *RMSE*. Although the RF model does not consider spatially non-stationary aspects, it can improve the prediction accuracy by gathering a large number of classification trees to find the relationship among variables [38]. In this study, the explanatory variables of fire occurrence were multiple, and the RF model precisely captured their relationship.

4.3. Model Comparison in Predictive Ability

In the last decades, model comparisons have evoked widespread attention to choosing the most suitable prediction models [31,37,39,40]. In our study, the GLR model's goodness of fit was not competitive with that of the other two models (GWLR and RF) (Table 4). Our results are consistent with previous fire-prediction studies [26,39,40], demonstrating that GWLR and RF perform better than GLR in predicting fire occurrences. Moreover, the GLR model improperly predicted a high probability of fire occurrences during winter at both locations (Figure 8a,c). The temporal distribution of historical fire occurrences showed only that fewer fires occurred in winter (Figure 5), suggesting that the prediction ability of the GLR model was not ideal in our study area. This may have been caused by other crucial environmental variables we did not consider, such as water deficit [78], drought [79] etc., demonstrating a need to explore further in future studies.

The GWLR model is an improvement over GLR by adding a spatial weight matrix to reduce model residuals [80], and therefore the goodness of fit was better than with GLR (Table 5). However, the GWLR model also erroneously predicted a high probability of fire occurrences during winter and summer at both locations (Figure 7a,c), contrary to the historical fire statistics (Figure 5). We speculated that the GWLR model focuses excessively on more significant meteorological variables and ignores the effects of other variables on fire occurrence.

The RF model had the best fit among the three models (Table 4). Moreover, the predictions for the two locations generally captured the seasonality of fire probability in our study area. Seasonal characteristics here were higher during spring and autumn and lower in winter and summer [81]. The predictions were also consistent with the fire prevention periods (Figure 8). Therefore, the RF model can be used to predict grassland-fire occurrences in our study area.

4.4. Factors Affecting Grassland-Fire Occurrences

Many factors may impact fire occurrences, including vegetation, meteorological/climatic factors, topography, and human activities [41,82,83]. In our study, meteorological/climatic factors (daily average specific humidity, daily average wind speed and mean annual temperature) showed a higher importance as revealed by the GWLR models, in line with previous studies [63,84]. Daily average specific humidity had a negative relationship to fire

occurrences (Tables 2 and 3) because, with the increase of air humidity, the fuel moisture content also increases, making the fuel hard to ignite [85]. However, the importance of daily average specific humidity had great spatial variations. More importance was observed in the eastern region (Figure 6a), which is near the sea, so the spatial difference of daily average humidity was more obvious.

Generally speaking, the higher the wind speed, the more water vapor produced by plant transpiration is taken away, and the more oxygen is brought to the combustion of fuels [86], thereby increasing the probability of fire occurrences. Therefore, in this study, the daily average wind speed was positively related to fire occurrences (Table 2). However, this positive correlation was not spatially uniform, with some parts of the central area showing a negative correlation (Figure 6b). We speculated that this may be due to the characteristics of a temperate continental monsoon climate. When the wind blows from the sea to the continent, it brings a humid airflow, thereby reducing the probability of fire occurrences.

Generally speaking, temperature correlated positively with fire occurrences [87]. On the contrary, a negative relation emerged in our study (Tables 2 and 3) because of the climate characteristics of rain and heat synchronization. When the moisture is high, fuel does not ignite easily in hot weather. Furthermore, this negative relation was also spatially non-stationary. In some parts of eastern Inner Mongolia, a significant difference is observed (Figure 6c) due to the greater differences of natural geographic features and cultural landscapes in our study area [26,79].

Concerning anthropogenic factors, the three significant human-related variables were, as expected, all negatively correlated with fire occurrence (Tables 2 and 3). Our results were consistent with previous research [28]. Historical fire records showed that the majority of fires were human originated. Human activities are more common near roads, settlements and rivers, resulting in more fire occurrences [63]. Therefore, human factors revealed a negative relation with fire occurrences. These relations were also spatially heterogeneous (Figure 6g–i) due to the variations in the spatial distribution of roads, rivers and settlements.

As for vegetation conditions, fuel moisture and fuel loads have crucial impacts on fire occurrences [22,69,88]. We found that the global vegetation moisture index (GVMI) was negatively correlated with fire occurrence (Tables 2 and 3) because with the increase of moisture, fuel is hard to ignite [26]. In addition, significant coefficients of GVMI were found in the eastern region (Figure 5d). This could be explained by the climate constraints hypothesis [89] as the fuel in the eastern region is abundant, and climate conditions determine fire occurrences. Our results also showed that NDVI was positively correlated with fire occurrences (Tables 2 and 3), for sufficient fuel is one of the burning conditions [84]. Spatially, however, only a small part of western Inner Mongolia had significant NDVI coefficients (Figure 6e), which may support the fuel constraints hypothesis [89]. Vegetation in western Inner Mongolia is sparse, but if coverage increases, this would significantly increase the fire-occurrence probability.

Finally, topographic factors also affect fire occurrence patterns [88,90]. In this study, we found that the slope and fire occurrence showed a negative correlation in some parts (Tables 2 and 3). Our results were consistent with the results obtained by Zhang [69]. We believe this emerged because the grasslands of Inner Mongolia are mainly distributed on a flat plateau; thus more grassland fires also occur on the flat ground, where there are limited slopes, resulting in a negative correlation between grassland-fire occurrences and slope.

4.5. Implications for Grassland Fire Management

From a spatial perspective, our results also showed spatial non-stationarities for various variables in predicting fire occurrences. For example, the influence of Humi_dy, Wind_dy, GVMI and D_resp on fire occurrences was significant in eastern Inner Mongolia, and NDVI, D_resp and D_river were important in western Inner Mongolia (Figure 5). The spatial non-stationarity of variables may have implications for accurately mapping fire risk zones for fire management based on different environmental factors for various regions, instead of traditional mapping methods which regard a variable as having equal

importance across a studied area. Furthermore, our results showed that the RF model performed best in our study area; consequently, this model should be used to map fire-occurrence probability. The spatial pattern of the probability of fire occurrence is of crucial importance in fire management [91]. This method could be applied to allocate priority areas for grassland fuel treatments [92]. From a temporal perspective, the fire-prevention period in spring and autumn should be adjusted according to local conditions. For example, Point 1, located on Hulunbuir region, has a high latitude and insufficient heat. According to the RF model prediction, the period of high fire probability in autumn starts and ends earlier than currently believed, and the period of high fire probability in spring is shorter (Figure 7a). Therefore, the fire prevention period should be adjusted accordingly.

Strict measures should be taken to prevent fires from occurring, such as forbidding any uses of wildland fire during fire-prevention periods and adding remote sensing data about grassland fuels into the original fire-monitor systems based on meteorological factors to improve prediction accuracy. In addition, with the increasing intensity of human activities, a large area of grassland is occupied by cultivated land, and increasingly burning straw in agriculture poses a fire danger. With global warming, the drivers of grassland fires become more complex. Grassland management strategies must pay more attention to changes in these drivers and their relationship with grassland fires to ensure effective fire prevention.

5. Conclusions

This study analyzed the temporal and spatial characteristics and driving factors of grassland fires in the Inner Mongolia Autonomous Region from 2000 to 2018, comparing the prediction accuracy of global logistic regression, geographically weighted logistic regression, and random forest models. The spatial distribution of historical fires in Inner Mongolian grasslands was higher in the east than in central and western areas, and the high-incidence fire season was generally the same as the fire-prevention period regulated for Inner Mongolian forests and grasslands. The quality fit of the random forest model was the highest, and geographically weighted logistic regression models were also significant to some extent for reference. The influence of nine drivers selected by a geographically weighted logistic-regression model on grassland fires was spatially unbalanced. The random forest and geographically weighted logistic-regression models both demonstrated that meteorological factors and NDVI were of great importance to grassland fires. Inner Mongolia has a vast territory, and different areas present different sensitivities to different drivers. Areas with different hydrothermal conditions had different fire-prevention periods; thus, grassland fire management strategies based on local conditions should be advocated. It is suggested to improve the existing methods of meteorological fire monitoring by adding remote sensing data of grassland fuels.

Author Contributions: Conceptualization, C.C. and Y.C.; methodology, C.C. and Y.C.; software, C.C. and Z.X.; validation, C.C.; formal analysis, C.C. and X.P.; investigation, M.G.; resources, H.Z.; data curation, C.C. and X.P.; writing—original draft preparation, C.C.; writing—review and editing, C.C. and Y.C.; visualization, C.C.; supervision, Y.H.; project administration, Y.C.; funding acquisition, Y.C. All authors have read and agreed to the published version of the manuscript.

Funding: This research was funded by the National Key Research and Development Program of China Strategic International Cooperation in Science and Technology Innovation Program (2018YFE0207800), the National Natural Science Foundation of China (grant no. 31971483), and the National Key R&D Program of China (Grant number: 2022YFC3003101).

Data Availability Statement: Not applicable.

Conflicts of Interest: The authors declare no conflict of interest.

References

1. Steiner, J.L.; Wetter, J.; Robertson, S.; Teet, S.; Wang, J.; Wu, X.; Zhou, Y.; Brown, D.; Xiao, X. Grassland Wildfires in the Southern Great Plains: Monitoring Ecological Impacts and Recovery. *Remote Sens.* **2020**, *12*, 619. [CrossRef]
2. Jiang, L.; Yu, S.; Wulantuya; Duwala. Summary of Grassland Fire Research. *Acta Agrestia Sin.* **2018**, *26*, 791–803.
3. Thomson, D.M.; Bonapart, A.D.; King, R.A.; Schultz, E.L.; Startin, C.R.; Ward, D. Long-term monitoring of a highly invaded annual grassland community through drought, before and after an unintentional fire. *J. Veg. Sci.* **2020**, *31*, 307–318. [CrossRef]
4. Bond, W.J.; Keeley, J.E. Fire as a global 'herbivore': The ecology and evolution of flammable ecosystems. *Trends Ecol. Evol.* **2005**, *20*, 387–394. [CrossRef] [PubMed]
5. Lamont, B.B.; He, T. Fire-Proneness as a Prerequisite for the Evolution of Fire-Adapted Traits. *Trends Plant Sci.* **2017**, *22*, 278–288. [CrossRef]
6. Chandra, K.K.; Bhardwaj, A.K. Incidence of forest fire in India and its effect on terrestrial ecosystem dynamics, nutrient and microbial status of soil. *Int. J. Agric. For.* **2015**, *5*, 69–78.
7. Jolly, W.M.; Cochrane, M.A.; Freeborn, P.H.; Holden, Z.A.; Brown, T.J.; Williamson, G.J.; Bowman, D.M.J.S. Climate-induced variations in global wildfire danger from 1979 to 2013. *Nat. Commun.* **2015**, *6*, 7537. [CrossRef]
8. Mohajane, M.; Costache, R.; Karimi, F.; Pham, Q.B.; Essahlaoui, A.; Nguyen, H.; Laneve, G.; Oudija, F. Application of remote sensing and machine learning algorithms for forest fire mapping in a Mediterranean area. *Ecol. Indic.* **2021**, *129*, 107869. [CrossRef]
9. Yu, T.; Zhuang, Q. Quantifying global N2O emissions from natural ecosystem soils using trait-based biogeochemistry models. *Biogeosciences* **2019**, *16*, 207–222. [CrossRef]
10. Podur, J.; Martell, D.L.; Csillag, F. Spatial patterns of lightning-caused forest fires in Ontario, 1976–1998. *Ecol. Model.* **2003**, *164*, 1–20. [CrossRef]
11. Adámek, M.; Jankovská, Z.; Hadincová, V.; Kula, E.; Wild, J. Drivers of forest fire occurrence in the cultural landscape of Central Europe. *Landsc. Ecol.* **2018**, *33*, 2031–2045. [CrossRef]
12. Zheng, W.; Shao, J.; Wang, M.; Liu, C. Dynamic monitoring and analysis of grassland fire based on multi-source satellite remote sensing data. *J. Nat. Disasters* **2013**, *22*, 54–61.
13. Sharma, S.; Dhakal, K. Boots on the Ground and Eyes in the Sky: A Perspective on Estimating Fire Danger from Soil Moisture Content. *Fire* **2021**, *4*, 45. [CrossRef]
14. Rakhmatulina, E.; Stephens, S.; Thompson, S. Soil moisture influences on Sierra Nevada dead fuel moisture content and fire risks. *For. Ecol. Manag.* **2021**, *496*, 119379. [CrossRef]
15. Vinodkumar, V.; Dharssi, I.; Yebra, M.; Fox-Hughes, P. Continental-scale prediction of live fuel moisture content using soil moisture information. *Agric. For. Meteorol.* **2021**, *307*, 108503. [CrossRef]
16. Van Linn, P.F.; Nussear, K.E.; Esque, T.C.; DeFalco, L.A.; Inman, R.D.; Abella, S.R. Estimating wildfire risk on a Mojave Desert landscape using remote sensing and field sampling. *Int. J. Wildland Fire* **2013**, *22*, 770–779. [CrossRef]
17. Bian, H.F.; Zhang, H.Y.; Zhou, D.W.; Xu, J.W.; Zhang, Z.X. Integrating models to evaluate and map grassland fire risk zones in Hulunbuir of Inner Mongolia, China. *Fire Saf. J.* **2013**, *61*, 207–216. [CrossRef]
18. Verbesselt, J.; Somers, B.; van Aardt, J.; Jonckheere, I.; Coppin, P. Monitoring herbaceous biomass and water content with SPOT VEGETATION time-series to improve fire risk assessment in savanna ecosystems. *Remote Sens. Environ.* **2006**, *101*, 399–414. [CrossRef]
19. Alexandre, P.M.; Mockrin, M.H.; Stewart, S.I.; Hammer, R.B.; Radeloff, V.C. Rebuilding and new housing development after wildfire. *Int. J. Wildland Fire* **2015**, *24*, 138–149. [CrossRef]
20. Oliveira, S.; Oehler, F.; San-Miguel-Ayanz, J.; Camia, A.; Pereira, J.M.C. Modeling spatial patterns of fire occurrence in Mediterranean Europe using Multiple Regression and Random Forest. *For. Ecol. Manag.* **2012**, *275*, 117–129. [CrossRef]
21. Mitchener, L.J.; Parker, A.J. Climate, lightning, and wildfire in the national forests of the southeastern United States: 1989–1998. *Phys. Geogr.* **2005**, *26*, 147–162. [CrossRef]
22. Wu, Z.W.; He, H.S.; Keane, R.E.; Zhu, Z.; Wang, Y.; Shan, Y. Current and future patterns of forest fire occurrence in China. *Int. J. Wildland Fire* **2020**, *29*, 104–119. [CrossRef]
23. Zapata-Rios, X.; Lopez-Fabara, C.; Navarrete, A.; Torres-Paguay, S.; Flores, M. Spatiotemporal patterns of burned areas, fire drivers, and fire probability across the equatorial Andes. *J. Mt. Sci.* **2021**, *18*, 952–972. [CrossRef]
24. Pavlek, K.; Biscevic, F.; Furcic, P.; Grdan, A.; Gugic, V.; Malesic, N.; Moharic, P.; Vragovic, V.; Fuerst-Bjelis, B.; Cvitanovic, M. Spatial patterns and drivers of fire occurrence in a Mediterranean environment: A case study of southern Croatia. *Geogr. Tidsskr.* **2017**, *117*, 22–35. [CrossRef]
25. Lafon, C.W.; Grissino-Mayer, H.D. Spatial patterns of fire occurrence in the central Appalachian mountains and implications for wildland fire management. *Phys. Geogr.* **2007**, *28*, 1–20. [CrossRef]
26. Su, Z.; Zheng, L.; Luo, S.; Tigabu, M.; Guo, F. Modeling wildfire drivers in Chinese tropical forest ecosystems using global logistic regression and geographically weighted logistic regression. *Nat. Hazards* **2021**, *108*, 1317–1345. [CrossRef]
27. Syphard, A.D.; Radeloff, V.C.; Keeley, J.E.; Hawbaker, T.J.; Clayton, M.K.; Stewart, S.I.; Hammer, R.B. Human influence on California fire regimes. *Ecol. Appl.* **2007**, *17*, 1388–1402. [CrossRef]
28. Liu, Z.; Yang, J.; Chang, Y.; Weisberg, P.J.; He, H.S. Spatial patterns and drivers of fire occurrence and its future trend under climate change in a boreal forest of Northeast China. *Glob. Chang. Biol.* **2012**, *18*, 2041–2056. [CrossRef]

29. Miranda, B.R.; Sturtevant, B.R.; Stewart, S.I.; Hammer, R.B. Spatial and temporal drivers of wildfire occurrence in the context of rural development in northern Wisconsin, USA. *Int. J. Wildland Fire* **2012**, *21*, 141–154. [CrossRef]
30. Wu, Z.; He, H.S.; Yang, J.; Liu, Z.; Liang, Y. Relative effects of climatic and local factors on fire occurrence in boreal forest landscapes of northeastern China. *Sci. Total Environ.* **2014**, *493*, 472–480. [CrossRef]
31. Phelps, N.; Woolford, D.G. Comparing calibrated statistical and machine learning methods for wildland fire occurrence prediction: A case study of human-caused fires in Lac La Biche, Alberta, Canadac. *Int. J. Wildland Fire* **2021**, *30*, 850–870. [CrossRef]
32. Graham, M.H. Confronting multicollinearity in ecological multiple regression. *Ecology* **2003**, *84*, 2809–2815. [CrossRef]
33. Zhang, H.; Han, X.; Dai, S. Fire Occurrence Probability Mapping of Northeast China with Binary Logistic Regression Model. *IEEE J. Sel. Top. Appl. Earth Obs. Remote Sens.* **2013**, *6*, 121–127. [CrossRef]
34. Fotheringham, A.S.; Brunsdon, C.; Charlton, M.E. *Geographically Weighted Regression: The Analysis of Spatially Varying Relationships*; John Wiley & Sons Ltd.: Chichester, UK, 2002.
35. Liang, H.; Wang, W.; Guo, F.; Lin, F.; Lin, Y. Comparing the application of logistic and geographically weighted logistic regression models for Fujian forest fire forecasting. *Acta Ecol. Sin.* **2017**, *37*, 4128–4141.
36. Rodrigues, M.; de la Riva, J. An insight into machine-learning algorithms to model human-caused wildfire occurrence. *Environ. Model. Softw.* **2014**, *57*, 192–201. [CrossRef]
37. De Vasconcelos, M.J.P.; Silva, S.; Tome, M.; Alvim, M.; Pereira, J. Spatial prediction of fire ignition probabilities: Comparing logistic regression and neural networks. *Photogramm. Eng. Remote Sens.* **2001**, *67*, 73–81.
38. Gao, C.; Lin, H.-L.; Hu, H.-Q.; Song, H. A review of models of forest fire occurrence prediction in China. *Ying Yong Sheng Tai Xue Bao = J. Appl. Ecol.* **2020**, *31*, 3227–3240. [CrossRef]
39. Guo, F.; Wang, G.; Su, Z.; Liang, H.; Wang, W.; Lin, F.; Liu, A. What drives forest fire in Fujian, China? Evidence from logistic regression and Random Forests. *Int. J. Wildland Fire* **2016**, *25*, 505–519. [CrossRef]
40. Phelps, N.; Woolford, D.G. Guidelines for effective evaluation and comparison of wildland fire occurrence prediction models. *Int. J. Wildland Fire* **2021**, *30*, 225–240. [CrossRef]
41. Parajuli, A.; Gautam, A.P.; Sharma, S.P.; Bhujel, K.B.; Sharma, G.; Thapa, P.B.; Bist, B.S.; Poudel, S. Forest fire risk mapping using GIS and remote sensing in two major landscapes of Nepal. *Geomat. Nat. Hazards Risk* **2020**, *11*, 2569–2586. [CrossRef]
42. Mallinis, G.; Petrila, M.; Mitsopoulos, I.; Lorent, A.; Neagu, S.; Apostol, B.; Gancz, V.; Popa, I.; Goldammer, J.G. Geospatial Patterns and Drivers of Forest Fire Occurrence in Romania. *Appl. Spat. Anal. Policy* **2019**, *12*, 773–795. [CrossRef]
43. Arnan, X.; Quevedo, L.; Rodrigo, A. Forest fire occurrence increases the distribution of a scarce forest type in the Mediterranean Basin. *Acta Oecol.* **2013**, *46*, 39–47. [CrossRef]
44. Matin, M.A.; Chitale, V.S.; Murthy, M.S.R.; Uddin, K.; Bajracharya, B.; Pradhan, S. Understanding forest fire patterns and risk in Nepal using remote sensing, geographic information system and historical fire data. *Int. J. Wildland Fire* **2017**, *26*, 276–286. [CrossRef]
45. Renard, Q.; Pélissier, R.; Ramesh, B.R.; Kodandapani, N. Environmental susceptibility model for predicting forest fire occurrence in the Western Ghats of India. *Int. J. Wildland Fire* **2012**, *21*, 368–379. [CrossRef]
46. Wotton, B.M.; Nock, C.A.; Flannigan, M.D. Forest fire occurrence and climate change in Canada. *Int. J. Wildland Fire* **2010**, *19*, 253–271. [CrossRef]
47. Muro, J.; Linstädter, A.; Magdon, P.; Wöllauer, S.; Männer, F.A.; Schwarz, L.-M.; Ghazaryan, G.; Schultz, J.; Malenovský, Z.; Dubovyk, O. Predicting plant biomass and species richness in temperate grasslands across regions, time, and land management with remote sensing and deep learning. *Remote Sens. Environ.* **2022**, *282*, 113262. [CrossRef]
48. Liu, M.; Dries, L.; Heijman, W.; Huang, J.; Zhu, X.; Hu, Y.; Chen, H. The Impact of Ecological Construction Programs on Grassland Conservation in Inner Mongolia, China. *Land Degrad. Dev.* **2018**, *29*, 326–336. [CrossRef]
49. Le Page, Y.; Pereira, J.M.C.; Trigo, R.; da Camara, C.; Oom, D.; Mota, B. Global fire activity patterns (1996-2006) and climatic influence: An analysis using the World Fire Atlas. *Atmos. Chem. Phys.* **2008**, *8*, 1911–1924. [CrossRef]
50. Jia, Y.; Cui, X.; Liu, Y.; Liu, Y.; Xu, C.; Li, T.; Ran, Q.; Wang, Y. Drought vulnerability assessment in Inner Mongolia. *Acta Ecol. Sin.* **2020**, *40*, 9070–9082.
51. Li, J.; Feng, C. Ecosystem service values and ecological improvement based on land use change: A case study of the Inner Mongolia Autonomous Region. *Acta Ecol. Sin.* **2019**, *39*, 4741–4750.
52. Zhou, H.; Wang, Y.; Zhou, G. Temporal and spatial dynamics of grassland fires in Inner Mongolia. *Acta Pratacult. Sin.* **2016**, *25*, 16–25.
53. Wheeler, D.C. Diagnostic tools and a remedial method for collinearity in geographically weighted regression. *Environ. Plan. A Econ. Space* **2007**, *39*, 2464–2481. [CrossRef]
54. Guo, F.; Su, Z.; Wang, G.; Sun, L.; Lin, F.; Liu, A. Wildfire ignition in the forests of southeast China: Identifying drivers and spatial distribution to predict wildfire likelihood. *Appl. Geogr.* **2016**, *66*, 12–21. [CrossRef]
55. Catry, F.X.; Rego, F.C.; Bação, F.L.; Moreira, F. Modeling and mapping wildfire ignition risk in Portugal. *Int. J. Wildland Fire* **2009**, *18*, 921–931. [CrossRef]
56. Engelmark, O. EARLY postfire tree regeneration in a Picea-Vaccinium forest in northern Sweden. *J. Veg. Sci.* **1993**, *4*, 791–794. [CrossRef]
57. Cardille, J.A.; Ventura, S.J.; Turner, M.G. Environmental and social factors influencing wildfires in the Upper Midwest, United States. *Ecol. Appl.* **2001**, *11*, 111–127. [CrossRef]

58. Diaz-Delgado, R.; Lloret, F.; Pons, X. Spatial patterns of fire occurrence in Catalonia, NE, Spain. *Landsc. Ecol.* **2004**, *19*, 731–745. [CrossRef]
59. Scholze, M.; Knorr, W.; Arnell, N.W.; Prentice, I.C. A climate-change risk analysis for world ecosystems. *Proc. Natl. Acad. Sci. USA* **2006**, *103*, 13116–13120. [CrossRef]
60. Shmuel, A.; Ziv, Y.; Heifetz, E. Machine-Learning-based evaluation of the time-lagged effect of meteorological factors on 10-hour dead fuel moisture content. *For. Ecol. Manag.* **2022**, *505*, 119897. [CrossRef]
61. Yang, K. *China Meteorological Forcing Data (1979–2018)*; National Tibetan Plateau/Third Pole Environment Data Center: Beijing, China, 2018. [CrossRef]
62. Vilar, L.; Woolford, D.G.; Martell, D.L.; Pilar Martin, M. A model for predicting human-caused wildfire occurrence in the region of Madrid, Spain. *Int. J. Wildland Fire* **2010**, *19*, 325–337. [CrossRef]
63. Chang, Y.; Zhu, Z.; Bu, R.; Chen, H.; Feng, Y.; Li, Y.; Hu, Y.; Wang, Z. Predicting fire occurrence patterns with logistic regression in Heilongjiang Province, China. *Landsc. Ecol.* **2013**, *28*, 1989–2004. [CrossRef]
64. Purevdorj, T.; Tateishi, R.; Ishiyama, T.; Honda, Y. Relationships between percent vegetation cover and vegetation indices. *Int. J. Remote Sens.* **1998**, *19*, 3519–3535. [CrossRef]
65. Jimenez-Munoz, J.C.; Sobrino, J.A.; Plaza, A.; Guanter, L.; Moreno, J.; Martinez, P. Comparison between Fractional Vegetation Cover Retrievals from Vegetation Indices and Spectral Mixture Analysis: Case Study of PROBA/CHRIS Data over an Agricultural Area. *Sensors* **2009**, *9*, 768–793. [CrossRef] [PubMed]
66. Ceccato, P.; Flasse, S.; Gregoire, J.M. Designing a spectral index to estimate vegetation water content from remote sensing data —Part 2 Validation and applications. *Remote Sens. Environ.* **2002**, *82*, 198–207. [CrossRef]
67. Syphard, A.D.; Radeloff, V.C.; Keuler, N.S.; Taylor, R.S.; Hawbaker, T.J.; Stewart, S.I.; Clayton, M.K. Predicting spatial patterns of fire on a southern California landscape. *Int. J. Wildland Fire* **2008**, *17*, 602–613. [CrossRef]
68. Conedera, M.; Torriani, D.; Neff, C.; Ricotta, C.; Bajocco, S.; Pezzatti, G.B. Using Monte Carlo simulations to estimate relative fire ignition danger in a low-to-medium fire-prone region. *For. Ecol. Manag.* **2011**, *261*, 2179–2187. [CrossRef]
69. Zhang, H. Spatial analysis of fire-influencing factors in Henan Province. *Prog. Geogr.* **2014**, *33*, 958–968.
70. Xu, X. *China Monthly Vegetation Index (NDVI) Spatial Distribution Dataset*; Chinese Academy of Sciences: Beijing, China, 2018. [CrossRef]
71. Mou, N.; Liu, W.; Wang, H.; Dai, H. *ArcGIS 10 Tutorial: From Beginner to Master*; Sinomap Press: Beijing, China, 2012. (In Chinese)
72. Nunes, A.N.; Lourenço, L.; Meira, A.C.C. Exploring spatial patterns and drivers of forest fires in Portugal (1980–2014). *Sci. Total Environ.* **2016**, *573*, 1190–1202. [CrossRef]
73. Su, H.; Shen, W.; Wang, J.; Ali, A.; Li, M. Machine learning and geostatistical approaches for estimating aboveground biomass in Chinese subtropical forests. *For. Ecosyst.* **2020**, *7*, 64. [CrossRef]
74. Karlson, M.; Ostwald, M.; Reese, H.; Sanou, J.; Tankoano, B.; Mattsson, E. Mapping Tree Canopy Cover and Aboveground Biomass in Sudano-Sahelian Woodlands Using Landsat 8 and Random Forest. *Remote Sens.* **2015**, *7*, 10017–10041. [CrossRef]
75. Jiménez-Valverde, A. Insights into the area under the receiver operating characteristic curve (AUC) as a discrimination measure in species distribution modelling. *Glob. Ecol. Biogeogr.* **2012**, *21*, 498–507. [CrossRef]
76. Xue, Z.C.; Kappas, M.; Wyss, D. Spatio-Temporal Grassland Development in Inner Mongolia after Implementation of the First Comprehensive Nation-Wide Grassland Conservation Program. *Land* **2021**, *10*, 38. [CrossRef]
77. Zhao, F.; Shu, L.; Di, X.; Tian, X.; Wang, M. Changes in the Occurring Date of Forest Fires in the Inner Mongolia Daxing'anling Forest Region Under Global Warming. *Sci. Silvae Sin.* **2009**, *45*, 166–172.
78. Syphard, A.D.; Sheehan, T.; Rustigian-Romsos, H.; Ferschweiler, K. Mapping future fire probability under climate change: Does vegetation matter? *PLoS ONE* **2018**, *13*, e0201680. [CrossRef]
79. Rodrigues, M.; Jiménez-Ruano, A.; Peña-Angulo, D.; de la Riva, J. A comprehensive spatial-temporal analysis of driving factors of human-caused wildfires in Spain using Geographically Weighted Logistic Regression. *J. Environ. Manag.* **2018**, *225*, 177–192. [CrossRef]
80. Monjarás-Vega, N.A.; Briones-Herrera, C.I.; Vega-Nieva, D.J.; Calleros-Flores, E.; Corral-Rivas, J.J.; López-Serrano, P.M.; Pompa-García, M.; Rodríguez-Trejo, D.A.; Carrillo-Parra, A.; González-Cabán, A.; et al. Predicting forest fire kernel density at multiple scales with geographically weighted regression in Mexico. *Sci. Total Environ.* **2020**, *718*, 137313. [CrossRef]
81. Shabbir, A.H.; Zhang, J.; Groninger, J.W.; van Etten, E.J.B.; Sarkodie, S.A.; Lutz, J.A.; Valencia, C. Seasonal weather and climate prediction over area burned in grasslands of northeast China. *Sci. Rep.* **2020**, *10*, 19961. [CrossRef]
82. Muller, M.M.; Vila-Vilardell, L.; Vacik, H. Towards an integrated forest fire danger assessment system for the European Alps. *Ecol. Inform.* **2020**, *60*, 101151. [CrossRef]
83. Sousa, D.; Cruz-Jesus, F.; Sousa, A.; Painho, M. A multivariate approach to assess the structural determinants of large wildfires: Evidence from a Mediterranean country. *Int. J. Wildland Fire* **2021**, *30*, 241. [CrossRef]
84. Guo, F.; Su, Z.; Wang, G.; Sun, L.; Tigabu, M.; Yang, X.; Hu, H. Understanding fire drivers and relative impacts in different Chinese forest ecosystems. *Sci. Total Environ.* **2017**, *605–606*, 411–425. [CrossRef]
85. Masinda, M.M.; Li, F.; Liu, Q.; Sun, L.; Hu, T. Prediction model of moisture content of dead fine fuel in forest plantations on Maoer Mountain, Northeast China. *J. For. Res.* **2021**, *32*, 2023–2035. [CrossRef]
86. Masinda, M.M.; Sun, L.; Wang, G.; Hu, T. Moisture content thresholds for ignition and rate of fire spread for various dead fuels in northeast forest ecosystems of China. *J. For. Res.* **2020**, *32*, 1147–1155. [CrossRef]

87. Syphard, A.D.; Rustigian-Romsos, H.; Mann, M.; Conlisk, E.; Moritz, M.A.; Ackerly, D. The relative influence of climate and housing development on current and projected future fire patterns and structure loss across three California landscapes. *Glob. Environ. Chang.* **2019**, *56*, 41–55. [CrossRef]
88. Naderpour, M.; Rizeei, H.M.; Ramezani, F. Forest Fire Risk Prediction: A Spatial Deep Neural Network-Based Framework. *Remote Sens.* **2021**, *13*, 2513. [CrossRef]
89. Krawchuk, M.A.; Moritz, M.A. Constraints on global fire activity vary across a resource gradient. *Ecology* **2011**, *92*, 121–132. [CrossRef]
90. Su, Z.W.; Tigabu, M.; Cao, Q.Q.; Wang, G.Y.; Hu, H.Q.; Guo, F.T. Comparative analysis of spatial variation in forest fire drivers between boreal and subtropical ecosystems in China. *For. Ecol. Manag.* **2019**, *454*, 117669. [CrossRef]
91. Sağlam, B.; Bilgili, E.; Durmaz, B.D.; Kadıoğulları, A.İ.; Küçük, Ö. Spatio-Temporal Analysis of Forest Fire Risk and Danger Using LANDSAT Imagery. *Sensors* **2008**, *8*, 3970–3987. [CrossRef]
92. Wei, Y.; Rideout, D.; Kirsch, A. An optimization model for locating fuel treatments across a landscape to reduce expected fire losses. *Can. J. For. Res.* **2008**, *38*, 868–877. [CrossRef]